Green Chemistry

Enhanced depolymerization of beech wood lignin and its removal with peroxidases through continuous separation of lignin fragments

ARTICLE

Enhanced depolymerization of beech wood lignin and its removal with peroxidases through continuous separation of lignin fragments

Kenneth Sze Kai Teo,[ab] Keiko Kondo,[acd] Kaori Saito,[de] Yu Iseki,[e] Takashi Watanabe,[de] Takashi Nagata,[abc]* Masato Katahira[abcd]*

Lignin valorization is indispensable for a green biorefinery. Enzymatic depolymerization using ligninolytic enzymes, like manganese and lignin peroxidases, is a promising approach. However, enzymatic depolymerization performed in a batch system is hindered by a repolymerization reaction. Here, we successfully enhanced the lignin depolymerization efficiency by performing peroxidase-catalyzed depolymerization of beech wood lignin in a recently reported membrane bioreactor, in which water-soluble lignin fragments are continuously passed through a membrane. The total amount of the water-soluble lignin fragments using the membrane bioreactor turned out to be maximally 28-fold higher than that with a batch bioreactor. GC-MS analysis showed the presence of a variety of short aliphatic and aromatic compounds as constituents of the water-soluble lignin fragments. Furthermore, lignin quantification of and SEC analyses of the remaining solid residue in the membrane bioreactor indicated a higher degree of lignin depolymerization and removal. Semi-quantitative NMR analysis also supported the effective lignin removal in the membrane bioreactor. These findings demonstrate the effectiveness of the membrane bioreactor for the enhancement of native lignin depolymerization and removal by peroxidases.

Introduction

At present, when environmental sustainability is a top-priority, the nonedible second-generation biomass has emerged as a promising carbon-neutral resource for replacing non-renewable fossil fuels. The woody biomass, a second-generation biomass packed with valuable organic compounds such as cellulose, hemicelluloses and lignin, is abundantly available on earth.[1] Recent consensus on the success of future biorefineries relies on the complete valorization of all these organic compounds in the biomass. Although high-value-added products from polysaccharides are extensively realized, lignin is heavily underutilized due to the absence of an economically feasible lignin depolymerization technique.[2] When an effective lignin depolymerization process is developed, a complete biorefinery process involving lignin valorization will result.

Lignin is a heterogeneous aromatic biopolymer that provides the functionalities of structural integrity, water transportation, and physical/chemical protection to plants.[3,4] Lignin is constructed through the random polymerization of three monolignols having guaiacyl (G), syringyl (S), and *p*-hydroxyphenyl (H) units through radical coupling.[5-7] The majority of interunit linkages found in native lignin are ether linkages, such as the β-O-4', 4-O-5', and α-O-4' ones, and the minority being carbon-carbon linkages, such as the β-5', β-β', β-1', and 5-5' ones.[6,8-10] The unsystematic and randomized lignin interunit linkages result in the high chemical recalcitrance of lignin. Hence, efficient lignin depolymerization involving the cleavage of these linkages is an imperative process to harness lignin for biochemical production.

Currently available lignin depolymerization processes can be classified into physical, chemical, and biological treatments.[11] Biological treatment exhibits excellent potential as it bypasses the need of harsh chemicals and reaction conditions. In nature, lignin is biologically degraded by microorganisms such as fungi and bacteria, fungi being the major lignin degraders. White-rot fungi are particularly intriguing as they are able to degrade lignin by secreting a variety of lignin-degrading enzymes, such as laccase, manganese peroxidase (MnP), lignin peroxidase (LiP), and versatile peroxidase (VP).[12-14] The laccase-mediator system has been widely lauded for its success in catalyzing degradation of lignin in various lignocellulosic biomasses.[15-20] However, high enzyme loading and a pressurized reactor with oxygen gas, which is needed for the laccase-mediator system, are undesirable from both sustainability and safety perspectives.

The catalytic activities of MnP, LiP, and VP toward phenolic and non-phenolic lignin were proved by using model dimer

a. Institute of Advanced Energy, Kyoto University, Gokasho, Uji, Kyoto 611-0011, Japan

b. Graduate School of Energy Science, Kyoto University, Gokasho, Uji, Kyoto 611-0011, Japan

c. Integrated Research Center for Carbon Negative Science, Institute of Advanced Energy, Kyoto University, Gokasho, Uji, Kyoto 611-0011, Japan

d. Biomass Product Tree Industry-Academia Collaborative Research Laboratory, Kyoto University, Gokasho, Uji, Kyoto 611-0011, Japan

e. Research Institute for Sustainable Humanosphere, Kyoto University, Gokasho, Uji, Kyoto 611-0011, Japan

*E-mail: katahira.masato.6u@kyoto-u.ac.jp, nagata.takashi.6w@kyoto-u.ac.jp

†Electronic Supplementary Information (ESI) available: See DOI: 10.1039/x0xx00000x

substrates.[21-23] In addition, a recent study reported by Majeka *et al.*[24] and Liu *et al.*[25] demonstrated that LiP successfully catalyzed degradation of technical lignin and lignin extracted from corn stover, respectively.

Although there has been remarkable progress in the research on MnP, LiP, and VP, there is still limited documentation on successful attempts of lignin depolymerization in a natural woody biomass by MnP, LiP, and VP. One of the major obstacles for lignin depolymerization by MnP, LiP, and VP, as well as by laccase-mediator system, is the co-occurrence of lignin depolymerization and repolymerization reactions.[26,27] The radical formation catalyzed by MnP, LiP, and VP, as well as by laccase-mediator system, leads to either the cleavage of lignin interunit linkages or undesirable repolymerization of lignin fragments through free radical coupling. The occurrence of radical coupling seriously limits the efficacy of enzymatic depolymerization.[28,29]

To date, various ingenious strategies have been developed to improve the efficiency of lignin depolymerization, such as the stabilization or suppression of reactive intermediates using an auxiliary enzyme,[24] base-catalyst,[30] and solvent,[31,32] or by limiting the accessibility and mobility of reactive lignin moieties by performing the reaction in the solid-state.[33] Recently, a membrane bioreactor that was designed for a laccase-catalyzed reaction by Steinmetz *et al.* successfully shifted the technical lignin reaction from polymerization to depolymerization.[34] In the membrane bioreactor, reactive lignin fragments generated by laccase were continuously isolated from the reaction system, which reduced the repolymerization reaction and enhanced the efficiency of lignin depolymerization. This approach is expected to be favorable also for a peroxidase-catalyzed reaction. Here, the effects of lignin fragment isolation on not only lignin depolymerization but also lignin removal through the peroxidase-catalyzed reaction were examined using various analytical methods. It is also notable that the effect of the peroxidase-catalyzed reaction was examined for a natural woody biomass in this study.

Here, we investigate the benefit of separating lignin fragments for the peroxidase-catalyzed lignin depolymerization of a natural woody biomass, beech wood, by comparing the reaction in a conventional batch bioreactor and that in the membrane bioreactor. For the reaction, heterologously-expressed white-rot fungal peroxidases, MnP of *Ceriporiopsis subvermispora* (also known as *Gelatoporia subvermispora*) and LiP of *Phanerochaete chrysosporium*, were used. Oxidative activity of MnP towards phenolic compounds was demonstrated,[35] while oxidative activities of LiP towards phenolic and non-phenolic compounds were demonstrated.[27] In order for a sustainable and economical approach, both enzymes are used without any chromatographic purification and the reaction is performed at room temperature with a low enzyme dosage (2 U per 1 g of beech wood).

Size-exclusion chromatography (SEC) analysis of the products released into the aqueous phase demonstrated a tremendous increase in the total amount of water-soluble lignin fragments attained by using the membrane bioreactor. Gas chromatography-mass spectrometry (GC-MS) analysis on the fragments revealed the presence of a variety of short aliphatic and aromatic compounds as constituents.

Then, the solid residues in the reaction vessels for batch and membrane bioreactors were analyzed. Lignin quantification by Klason lignin and UV-Vis spectroscopic methods indicated the enhanced lignin removal for the membrane bioreactor. Furthermore, the SEC analysis demonstrated the significant enhancement of lignin depolymerization achieved by applying the membrane bioreactor, which results in an increase in the yield of low molecular weight lignin. Additionally, two-dimensional nuclear magnetic resonance spectroscopy (2D NMR) also supported the significant lignin removal from the solid residues for the membrane bioreactor.

Overall, this study demonstrated remarkable improvement in peroxidase-catalyzed depolymerization of beech wood lignin when performed in the membrane bioreactor as opposed to the batch bioreactor. Isolation of highly reactive lignin fragments is suggested to be the key to accomplish greater lignin depolymerization of a native biomass without the requirement of harsh chemicals or solvents.

Experimental

Methods

Preparation of milled beech wood. Beech wood chips (Shinseisangyo, Japan) were pulverized and sieved to a particle size of less than 40-mesh. After being Soxhlet-extracted with acetone for 24 h, the wood powder was dried overnight at 40 °C. The resulting powder was ball-milled using a Fritsch P-6 planetary mono mill, 1 g of the sample being added to an 80 mL agate jar containing 100 g of 3 mm ZrO_2 beads. The milling was performed under a nitrogen environment at 550 rpm for 1.5 h (90 cycles of 1 min milling with 1 min intervals). The milled solid was repeatedly washed with Milli-Q at a loading of 5% (w/w) until a near-colorless supernatant was obtained, which was lyophilized to yield MBW.

Preparation of crude MnP and LiP. MnP and LiP were expressed in *Pichia pastoris*. The details of the preparation procedure are described in Supplementary Method S1. The enzymatic activities of the obtained crude MnP and crude LiP were assayed using 2,6-dimethoxyphenol as a substrate. The enzymatic reaction was performed at 25 °C for 30 min. The formation of the product (coerulignone) was monitored spectroscopically as the increase in the visible light absorbance at 469 nm using Infinite® 200 PRO (TECAN). One unit of peroxidase activity was defined as the formation of 1 µmol of coerulignone ($\varepsilon_{469\ nm} = 53.2$ mM^{-1} cm^{-1}) per min. Peroxidase was prepared freshly before each enzymatic reaction.

Peroxidase-catalyzed lignin degradation in the batch bioreactor. Peroxidase-catalyzed reactions for MBW were carried out in screw-capped glass bottles containing 500 mg of MBW, 1 mM $MnSO_4$, and 2 U of either MnP or LiP (Fig. 1a). The total volume of the solution was adjusted to 200 mL with sodium malonate (pH 4.5). The air in the bottle was replaced with nitrogen gas to mimic the environment in the later mentioned membrane bioreactor. The enzymatic reaction was

initiated by the addition of hydrogen peroxide (H_2O_2) at 0.2 mM and conducted with magnetic stirring at room temperature. After four hours, fresh H_2O_2 (half of the original dose, i.e., 0.1 mM) was added followed by incubation for another four hours. In control experiments, the same procedures were performed with solutions, that did not contain either peroxidase or MBW. After eight hours of incubation, a supernatant and solid residue (RES_{batch}) were separated by centrifugation. The supernatant was frozen until analysis. The RES_{batch} obtained for MnP (RES_{batch}^{MnP}), LiP (RES_{batch}^{LiP}), and without peroxidases ($RES_{batch}^{no\ enzyme}$), were washed with Milli-Q by repeated suspension at a loading of 2% (w/w) and centrifugation (4,400 × g for 10 min) until a near-colorless supernatant was obtained, which was lyophilized.

Peroxidase-catalyzed lignin degradation in the membrane bioreactor. Peroxidase-catalyzed reactions for MBW were also carried out in a membrane bioreactor, which comprised a 400 mL ultrafiltration stirred cell (Millipore 5124, Merck) equipped with a 3000 cut-off RC membrane disc (PLBC07610, Merck) with a diameter of 76 mm (Fig. 1b). The initial components of the reaction mixture were identical to those for the aforementioned batch bioreactor. The reaction was initiated by the addition of H_2O_2 at 0.2 mM and conducted with magnetic stirring at room temperature for eight hours. Immediately after starting the reaction, the surface of the reaction mixture was pressurized at 4 bars with nitrogen to enhance the filtration, the initial filtration rate being 80 mL h^{-1}. The filtrate passed through the RC membrane was fractionated every one-hour. Every one-hour, 80 mL of sodium malonate (pH 4.5) containing 1 mM $MnSO_4$ and 0.2 mM H_2O_2 was added to the reactor. In control experiments, the same procedures were performed with solutions that did not contain either peroxidase or MBW. The collected filtrates were frozen until further analysis. The solid fraction remaining in the membrane bioreactor ($RES_{membrane}$) was collected. The $RES_{membrane}$ obtained for MnP ($RES_{membrane}^{MnP}$), LiP ($RES_{membrane}^{LiP}$), and without peroxidases ($RES_{membrane}^{no\ enzyme}$), were washed with Milli-Q by repeated suspension at a loading of 2% (w/w) and centrifugation (4,400 × g for 10 min) until a near-colorless supernatant was obtained, which was lyophilized.

SEC of the products released into the aqueous phase. The products released into the aqueous phase in the batch and membrane bioreactors were subjected to SEC. The details of the SEC procedure are described in Supplementary Method S2. A series of polystyrene sulfonate sodium salt standards (peak molecular weight (M_p) = 891-65400), syringol (M_p = 154), and guaiacol (M_p = 124) were used as calibration standards. The calibration standards were used for estimating the molecular weight of the products.

The total amount of products detected at 18.8 min for the batch bioreactor (TA_{B_19}) was estimated with Eq. (1), where I_{B_19} the area of product peak detected at 18.8 min on SEC, and $V_{supernatant}$ the total volume of the supernatant collected from the batch bioreactor.

$$TA_{B\_19} = I_{B\_19} \times V_{supernatant} \qquad (1)$$

The total amount of products detected at 18.8 min for the membrane bioreactor (TA_{M_19}) was estimated with Eq. (2),

where i is the number of filtrate fraction collected every one hour, $I_{M\_19,i}$ the area of the product peak detected at 18.8 min on SEC for filtrate fraction i, and $V_{filtrate,i}$ the volume of fraction i.

$$TA_{M\_19} = \sum_i (I_{M\_19,i} \times V_{filtrate,i}) \qquad (2)$$

TA_{B_19} and TA_{M_19} have arbitrary units and are used to compare the amounts of products detected at 18.8 min on SEC.

GC-MS analysis of the depolymerized products in the filtrate. The depolymerized product (M_19) was collected based on the elution profile and then lyophilized. The resulting solid was dissolved in ethyl acetate and trimethylsilylated. Then, the trimethylsilylated sample was analyzed by GC-MS. The details of the GC-MS procedure are described in Supplementary Method S3. Putative identification of the lignin depolymerization products was established by comparing the mass spectra of the unknown components to those available in the NIST mass spectral library. Products with a similarity index above 80% were listed in Table 1.

Chemical composition analysis of the solid residues. The percentages of lignin (LPs) of MBW, RES_{batch}, and $RES_{membrane}$ were determined by both the Klason lignin method[16,36-37] and the UV-Vis spectroscopic method.[38] The quantification by both methods was performed in duplicate. The details of the Klason lignin method and the UV-Vis spectroscopic method are described in Supplementary Method S4.

On the basis of the LP value determined by either the Klason lignin or UV-Vis spectroscopic method, the change in LP for each sample was calculated according to the following Eq. (3),[39] where LP_0 is the initial LP of MBW, and LP the LP of each sample.

$$\text{Change in LP} = \frac{LP - LP_0}{LP_0} \times 100\% \qquad (3)$$

The cellulose and hemicellulose contents were determined using a HPLC system (Shimadzu, Japan) equipped with a refractive index detector (RID-20A, Shimadzu).[36-37] The details on the determination of cellulose and hemicellulose contents are described in Supplementary Method S4.

SEC for solid residues. The molecular weight distributions of lignin in MBW, RES_{batch}, and $RES_{membrane}$ were determined by SEC. Cellulolytic enzyme lignin (CEL) were obtained from the sample by treating the sample with cellulolytic enzyme cocktail. The obtained CEL was then acetylated and dissolved in tetrahydrofuran for SEC analysis. The details of the sample preparation and SEC procedure are described in Supplementary Method S5. A series of polystyrene standards (PStQuickC, weight average molecular weight (M_w) = 5970-2110000, Tosoh), 1-(3,4-Dimethoxyphenyl)-2-(2-methoxyphenoxy)-1,3-propanediol (M_w = 334), and vanillin (M_w = 152) were used to construct a calibration curve. M_w, number average molecular weight (M_n), and polydispersity index (PDI) were calculated using a LabSolutions software (Shimadzu).

Structural analysis of MBW solid residue by 2D NMR. The lignin substructures in MBW, RES_{batch}, and $RES_{membrane}$ were analyzed by the gel-state 2D NMR method described by Shawn *et al.*[40] Without performing cellulase treatment, 60 mg of the sample (RES_{batch} and $RES_{membrane}$) was transferred to a 5 mm NMR tube and swollen with 500 µL of DMSO-d$_6$ containing 0.4 mM deuterated 4,4-dimethyl-4-silapentane-1-sulfonic acid

(DSS-d_6). The sample was sonicated for 1-5 h, during which the temperature of the ultrasonic bath was maintained below 40 °C, to obtain a homogeneous gel. NMR spectra were recorded using a Bruker Avance III HD 600 MHz instrument equipped with a 5 mm cryogenic probe and Z gradient (Bruker BioSpin, MA, USA). Acquisition of 2D ^{1}H-^{13}C HSQC spectra was performed using a standard Bruker pulse sequence 'hsqcetgpsisp2.2' at 313 K. Signals were calibrated using DMSO as a reference (δC 39.5 ppm; δH 2.49 ppm). Data processing, signal assignment, and signal volume integration were performed with Bruker TopSpin 3.6.4 software. DSS-d_6 was used as the internal chemical shift and quantification reference; the volume of each signal was normalized as to the signal volume of DSS-d_6. A semi-quantitative analysis of the volume integrals of the HSQC correlation peaks was performed according to the literatures.[41-42] The contents of β-O-4', β-β', and β-5' interunit linkages were estimated from the volume of their C_α-H_α correlations in the aliphatic region. The contents of S- and S'-units were estimated from the half values of the volume of their $C_{2,6}$-$H_{2,6}$ correlations, whereas that of the G-unit was estimated from the volume of the C_2-H_2 correlation in the aromatic region. The signal assignments of the 2D NMR spectra were obtained according to the literatures.[16,41-43]

The relative amounts of lignin substructures per control was calculated with Eq. (4), where $\int S_{ctrl}$ is the HSQC integral for the lignin substructure for $RES_{batch}^{no\ enzyme}$ or $RES_{membrane}^{no\ enzyme}$ and $\int S_{RES}$ the HSQC integral for the lignin substructure for either RES_{batch}^{MnP}, RES_{batch}^{LiP}, $RES_{membrane}^{MnP}$, or $RES_{membrane}^{LiP}$.

$$\text{Relative amounts of lignin substructures per control} = \frac{\int S_{RES}}{\int S_{ctrl}} \times 100\% \quad (4)$$

Enzymatic hydrolysis of solid residues. The hydrolysis of MBW, RES_{batch}, and $RES_{membrane}$ was conducted using a commercial cellulolytic enzyme cocktail (CellicCtec2, Novozymes, Denmark). 5 mg of the lyophilized dried sample (MBW, RES_{batch}, and $RES_{membrane}$) was treated with 0.02 FPU of CellicCtec2 in 500 μL of 50 mM sodium citrate (pH 5) at 50 °C for 24 h with shaking. After the 24 h-incubation, the samples were centrifuged at 10,000 × g for 5 min to separate the hydrolysate. The amount of reducing sugar released in the hydrolysate was determined using the dinitro salicylic acid method, with glucose used as the standard for comparison and quantification.[44]

Results

Peroxidase-catalyzed lignin depolymerization in batch and membrane bioreactors

Milled beech wood (MBW), prepared by size reduction and extractives removal, was used as a natural lignocellulosic substrate for evaluating peroxidase-catalyzed lignin depolymerization using either a batch or membrane bioreactor. Crude MnP or LiP, which were heterologously expressed in *Pichia pastoris*, was used for this evaluation. The reaction using the batch or membrane bioreactor was performed for eight hours, as illustrated in Fig. 1. In the batch bioreactor (Fig. 1a), the enzymatic reaction proceeded without any separation of reaction components. 0.2 mM H_2O_2 was added at the beginning

and 0.1 mM after four hours of reaction for the batch bioreactor. On the other hand, in the reaction using the membrane bioreactor (Fig. 1b), low molecular weight components including depolymerized products were continuously separated from the reaction mixture by ultrafiltration through a regenerated cellulose (RC) membrane with a 3000 molecular weight cut off (MWCO). 80 mL of buffer containing 0.2 mM H_2O_2 and 1 mM $MnSO_4$ was added every hour of reaction for the membrane bioreactor. The pressure inside the membrane bioreactor was kept constant, the filtration rate remaining constant at around 80 mL h^{-1} throughout the reaction, indicating no fouling or clogging of the RC membrane.

Analysis of aromatic products released into the aqueous phase

Water-soluble products that were released into the aqueous phase through a peroxidase-catalyzed reaction were analyzed by SEC with UV absorbance detection at 280 nm. For the batch bioreactor, the water-soluble products were obtained from the supernatant of the reactant after 8 h incubation of MBW with either MnP (Fig. 2a, black line) or LiP (Fig. 2b, black line). In the case of both MnP and LiP, a peak (denoted as B_19 in Fig. 2) was detected at 18.8 min. As B_19 was not detected for the control sample, which was obtained by performing the experiments without either a peroxidase (Fig. 2a and 2b, cyan line) or MBW (Fig. 2c), B_19 is regarded as being a peak of a reaction product derived from MBW through a peroxidase-catalyzed reaction. The UV absorbance at 280 nm of the product indicated that it contains aromatic groups. This suggests that the product is a lignin fragment derived from MBW. Sulfonated polystyrene whose molecular weight is 894 appeared at 14.2 min in the same SEC experiment, while guaiacol whose molecular weight is 124 did at 21.0 min. This indicates that the molecular weights of products corresponding to B_19 are between 124 and 894. These results indicate that both MnP and LiP successfully catalyzed the depolymerization of MBW in the batch bioreactor and produced a water-soluble lignin fragment.

For the membrane bioreactor, the filtrate, which passed through the 3000 MWCO membrane during the depolymerization of MBW by either MnP or LiP, was collected every one-hour. The filtrate obtained after the first one-hour for either MnP (Fig. 2d, black line) or LiP (Fig. 2e, black line) was analyzed by SEC. In both chromatograms, a product peak (denoted as M_19) was detected at 18.8 min. A corresponding peak was not detected for the control sample, which was obtained by performing the experiment without either a peroxidase (Fig. 2d and 2e, cyan line) or MBW (Fig. 2f). M_19 was also detected in the filtrate fractions collected at following time points (Supplementary Figure S1). It was noticed that the retention time of M_19 matched that of B_19 detected in the case of the batch bioreactor. These results confirmed that a water-soluble lignin fragment with a molecular weight between 124 and 894 was also produced in the membrane bioreactor. This indicated that the water-soluble lignin fragment could be separated from the reaction system through the RC membrane over the course of the reaction. As the intensity of M_19 peak

decreased monotonically over the incubation time (Supplementary Figure S1), the reaction was suggested to occur mainly at an early stage of incubation.

The total amounts of the products detected at 18.8 min were quantified on the basis of their absorbance at 280 nm. The total amount of products at 18.8 min for the batch bioreactor, TA_{B_19}, was deduced using Eq. (1). The total amount of products at 18.8 min for the membrane bioreactor, TA_{M_19}, was deduced using Eq. (2). As the molar extinction coefficient differs for each product, only a rough estimation of amounts of products can be obtained by this method. TA_{M_19} reached 28-fold of TA_{B_19} in the case of the MnP-catalyzed reaction (Fig. 2g). Similarly, in the case of the LiP-catalyzed reaction, TA_{M_19} reached 18-fold of TA_{B_19} (Fig. 2g). Thus, in the cases of both MnP and LiP, the ability to produce water-soluble lignin fragments from MBW was significantly enhanced by applying continuous product separation using the membrane bioreactor.

Identification of the depolymerized products in the filtrate

To identify the products obtained after the depolymerization of MBW catalyzed either by MnP or LiP, we performed a GC-MS analysis. The depolymerized products in the filtrate fraction, M_19 (Fig. 2d and 2e), were concentrated and analyzed. We employed a similarity search approach by comparing the product spectrum with those available in the NIST mass spectra library, using a similarity index threshold of 80% or higher. The identified compounds are listed in Table 1.

For MnP-catalyzed depolymerization of MBW, an aliphatic compound (No. 3) and several aromatic compounds (No. 4-7) were identified. MnP-catalyzed reaction produced aromatic products like syringol and vanillin, which were subsequently isolated from the reaction vessel through the membrane.

For LiP-catalyzed depolymerization of MBW, a variety of aliphatic (No. 1-3) and aromatic (No. 4-5 and 7-8) compounds were identified. The products such as vanillin and veratryl aldehyde were produced from the LiP-catalyzed reaction and isolated from the reaction vessel.

It is worth nothing that syringol was obtained only for MnP-catalyzed depolymerization of MBW, whereas veratryl aldehyde was obtained only for LiP-catalyzed depolymerization of MBW. Furthermore, methylated compounds like No. 4, 5 and 7 were observed. Such methylated compounds have been reported in a study by Zhang *et al.*, where methyl vanillate, methyl 3-(3,5-di-tert-butyl-4-hydroxyphenyl)propionate, and veratryl alcohol were formed from the enzymatic hydrolysis of corn stover lignin using laccase, MnP and LiP.[45]

Lignin removal from MBW through the peroxidase-catalyzed reaction

As the release of water-soluble lignin fragments through the peroxidase-catalyzed reaction in the batch and membrane bioreactors was confirmed, we next calculated the percentages of lignin (LP) in the solid residues (RES) in the reaction vessels for the batch and membrane bioreactors, RES_{batch} and $RES_{membrane}$, respectively. Here, the LPs of RES_{batch} and $RES_{membrane}$ were quantified by a conventional Klason lignin

method and a recently reported UV-Vis spectroscopic method (Table 2).[38] Firstly, the LP of MBW before the reaction was found to be 24.5 ± 0.4 and 26.9 ± 0.3% by the Klason lignin and UV-Vis spectroscopic methods, respectively. In the case of the batch bioreactor, the LP of RES_{batch} obtained for MnP (RES_{batch}^{MnP}) decreased to 21.4 ± 0.6% (22.3 ± 0.7%) according to the Klason lignin method (UV-Vis spectroscopic method). The change in LP relative to MBW was calculated using Eq. (3) as being −12.6 ± 0.6% (−17.3 ± 1.7%) (Table 2 and Fig. 3). On the other hand, the LP of RES_{batch} obtained for LiP (RES_{batch}^{LiP}) decreased to 19.8 ± 0.3% (19.4 ± 0.9%) according to the Klason lignin method (UV-Vis spectroscopic method). The change in LP correspond to −19.2 ± 0.8% (−27.7 ± 2.5%). On the contrary, the LP of RES_{batch} of a control sample that was obtained for the experiment without a peroxidase ($RES_{batch}^{No\ enzyme}$) was much closer to the LP of MBW; the change in LP was −6.9 ± 0.8% (−0.4 ± 1.0%) according to the Klason lignin method (UV-Vis spectroscopic method). This indicates that the decreases of the LP of RES_{batch}^{MnP} and RES_{batch}^{LiP} were achieved through the catalytic activities of MnP and LiP. This indicates that both MnP and LiP could catalyze the lignin removal from MBW even in the batch bioreactor to some extent.

In the case of the membrane bioreactor, the LP of $RES_{membrane}$ obtained for MnP ($RES_{membrane}^{MnP}$) was 16.9 ± 0.6% (16.2 ± 0.5%) according to the Klason lignin method (UV-Vis spectroscopic method); the change in LP corresponds to −31.1 ± 2.4% (−39.7 ± 1.7%). A comparison of the decrease in LP obtained for the batch bioreactor and membrane bioreactors showed that the latter is 2.5-fold (2.3-fold) more effective for MnP.

Meanwhile, the LP of $RES_{membrane}$ obtained for LiP ($RES_{membrane}^{LiP}$) was 14.3 ± 0.5% (14.2 ± 1.0%) according to the Klason lignin method (UV-Vis spectroscopic method); the change in LP corresponds to −41.5 ± 1.9% (−46.7 ± 3.4%). A comparison of the decrease in LP obtained for the batch and membrane bioreactors showed that the latter is 2.2-fold (1.7-fold) more effective for LiP. Therefore, the lignin removal from MBW catalyzed by both MnP and LiP using the membrane bioreactor significantly outperformed that with the batch bioreactor. Notably, the lignin removal was higher in the reaction catalyzed by LiP than that by MnP in both bioreactors.

Molecular weight distribution of lignin in the solid residues

Next, the distribution of the molecular weights of lignin contained in the solid fraction was investigated by SEC analysis. Firstly, cellulolytic enzyme lignin (CEL) was isolated through enzymatic digestion of polysaccharides from untreated MBW, RES_{batch}^{MnP}, RES_{batch}^{LiP}, $RES_{membrane}^{MnP}$, and $RES_{membrane}^{LiP}$, individually. Then the obtained CELs were acetylated. The molecular weight distribution of the acetylated CEL of MBW appeared to be bimodal (Fig. 4, cyan line). Similarly, the molecular weight distribution of the acetylated CELs of both RES_{batch}^{MnP} and RES_{batch}^{LiP} was also bimodal (Fig. 4, orange line). Therefore, we drew a line at a retention time corresponding to the molecular weight of 1000 in Fig. 4 (dotted line), and defined the fractions larger and smaller than 1000 as the high molecular

weight lignin (HML) and low molecular weight lignin (LML), respectively. The relative amount, or proportion, of HML and LML was estimated from the peak area of each fraction (Table 3). The proportion of HML in MBW was 88.2%. The proportions of HML for $\text{RES}_{\text{batch}}^{\text{MnP}}$ and $\text{RES}_{\text{batch}}^{\text{LiP}}$ turned out to be decreased to 68.0 and 74.3%, respectively. This is equivalent to the increases in the proportions of LML for $\text{RES}_{\text{batch}}^{\text{MnP}}$ and $\text{RES}_{\text{batch}}^{\text{LiP}}$ to 32.0 and 25.7%, respectively, from 11.8% for MBW. Such changes in the proportions of HML and LML were not observed for $\text{RES}_{\text{batch}}^{\text{No enzyme}}$, for which MBW was similarly incubated in the batch bioreactor without a peroxidase. Therefore, the peroxidase-catalyzed reaction led to a shift of the molecular-weight distribution from HML to LML, which indicates the depolymerization of HML had proceeded through a peroxidase-catalyzed reaction. Next, the weight-average molecular weight (M_w) of each fraction was calculated. The M_w of HML for $\text{RES}_{\text{batch}}^{\text{MnP}}$ and $\text{RES}_{\text{batch}}^{\text{LiP}}$ decreased to 7968 and 8501 g mol^{-1}, respectively, from 11336 g mol^{-1} for MBW, which also indicates the depolymerization of HML had proceeded through a peroxidase-catalyzed reaction. On the other hand, the M_w of LML was not drastically different before and after the reaction. The M_w of LML of around 230 g mol^{-1} is in the range of the molecular weights of monomeric and dimeric lignin units. Overall, both MnP and LiP were demonstrated to catalyze the lignin depolymerization in MBW even in the batch bioreactor.

Likewise, a bimodal-shaped molecular weight distribution was also observed in the case of the membrane bioreactor (Fig. 4, gray line). The proportions of HML for $\text{RES}_{\text{membrane}}^{\text{MnP}}$ and $\text{RES}_{\text{membrane}}^{\text{LiP}}$ turned out to be decreased to 62.6 and 49.0%, respectively, from 88.2% for MBW. This is equivalent to the increases in the proportions of LML for $\text{RES}_{\text{membrane}}^{\text{MnP}}$ and $\text{RES}_{\text{membrane}}^{\text{LiP}}$ to 37.4 and 51.0%, respectively, from 11.8% for MBW. Additionally, the M_w of HML for $\text{RES}_{\text{batch}}^{\text{MnP}}$ and $\text{RES}_{\text{batch}}^{\text{LiP}}$ decreased to 6155 and 6313 g mol^{-1}, respectively, from 11336 g mol^{-1} for MBW. It is apparent that the decreases in the proportion and M_w of HML were more drastic for the membrane bioreactor than for the batch bioreactor.

Analysis of lignin substructures in the solid residues by NMR spectroscopy

To obtain chemical and structural insights into lignin contained in untreated MBW, $\text{RES}_{\text{batch}}^{\text{MnP}}$, $\text{RES}_{\text{batch}}^{\text{LiP}}$, $\text{RES}_{\text{membrane}}^{\text{MnP}}$, and $\text{RES}_{\text{membrane}}^{\text{LiP}}$, we performed gel-state 2D ^{1}H-^{13}C heteronuclear single-quantum coherence (HSQC) analysis (Figs. 5 and 6). In the spectrum of $\text{RES}_{\text{batch}}^{\text{No enzyme}}$, typical signals of S-, G-, and α-oxidized S (S'-) units were detected in the aromatic region (Fig. 5a, upper panel). Meanwhile, typical signals of lignin interunit linkages, β-O-4', β-β', and β-5', and polysaccharide signals were detected in the aliphatic region (Fig. 5a, lower panel). No new peak was observed in the spectrum of either $\text{RES}_{\text{batch}}^{\text{MnP}}$ (Fig. 5b) or $\text{RES}_{\text{batch}}^{\text{LiP}}$ (Fig. 5c) when compared with the spectrum of $\text{RES}_{\text{batch}}^{\text{No enzyme}}$ (Fig. 5a). This suggests that there is no notable structural modification of either lignin or polysaccharide in the solid residues caused by the peroxidase-catalyzed reaction.

The contents of β-O-4', β-β', and β-5' interunit linkages were estimated from the volume of their C_α-H_α correlations in the aliphatic region (β-O-4' from A_α; β-β' from C_α; β-5' from B_α). Then, we expressed the amount of each interunit linkage as a fraction of the total lignin interunit linkages with reference to literatures (Supplementary Table S3).[41-42]

Next, relative amounts of lignin substructures (S-, G-, and S'-units, β-O-4' and some of the C-C' interunit linkages, C-C' (β-β' and β-5')) upon peroxidase-catalyzed reaction were estimated based on Eq. (4) (Fig. 7). In the case of $\text{RES}_{\text{batch}}^{\text{MnP}}$, the quantities of S-, G-, and S'- units decreased to 42, 30, and 64%, respectively, of those for $\text{RES}_{\text{batch}}^{\text{No enzyme}}$ (Fig. 7). The quantities of β-O-4' and C-C' interunit linkages decreased to 35 and 21%, respectively, of those for $\text{RES}_{\text{batch}}^{\text{No enzyme}}$ (Fig. 7). Likewise, in the case of $\text{RES}_{\text{batch}}^{\text{LiP}}$, the quantities of S-, G-, and S'- units decreased to 56, 43, and 70%, respectively (Fig. 7). The quantities of β-O-4' and C-C' interunit linkages decreased to 54 and 30%, respectively (Fig. 7). The decreases in the relative amounts of lignin substructures were suggested to be the result of lignin removal from MBW achieved due to the peroxidase-catalyzed reaction in the batch bioreactor.

We then analyzed the spectra of $\text{RES}_{\text{membrane}}$. No new peak was observed in the spectrum of either $\text{RES}_{\text{membrane}}^{\text{MnP}}$ (Fig. 6b) or $\text{RES}_{\text{membrane}}^{\text{LiP}}$ (Fig. 6c) when compared with the spectrum of $\text{RES}_{\text{membrane}}^{\text{No enzyme}}$ (Fig. 6a). Therefore, as was the case in the batch bioreactor, notable structural modification was not observed for either lignin or polysaccharide in the solid fractions.

As for the relative amounts of lignin substructures, the S-, G-, and S'- units for $\text{RES}_{\text{membrane}}^{\text{MnP}}$ decreased to 7, 1, and 1%, respectively, of those for $\text{RES}_{\text{membrane}}^{\text{No enzyme}}$ (Fig. 7). Whereas, the quantity of the β-O-4' interunit linkage decreased to 6% of that for $\text{RES}_{\text{membrane}}^{\text{No enzyme}}$, and those of C-C' interunit linkages were less than the detection limit (Fig. 7). In the case of $\text{RES}_{\text{membrane}}^{\text{LiP}}$, the quantities of the S-, G-, and S'- units decreased to 12, 3, and 5%, respectively (Fig. 7). Whereas, the quantity of the β-O-4' interunit linkage decreased to 10% and those of C-C' interunit linkages were less than the detection limit (Fig. 7). Overall, for both MnP and LiP, the reduction in the relative amounts of lignin substructures was much more pronounced for the membrane bioreactor than for the batch bioreactor, which may reflect the higher extent of lignin removal in the case of the membrane bioreactor.

Enzymatic hydrolysis of solid residues

To assess the hydrolysis efficiency following MnP- and LiP-catalyzed lignin depolymerization of MBW, we performed an enzymatic hydrolysis experiment using a commercial cellulase cocktail (CellicCtec2) and quantified the total reducing sugar content produced from the hydrolysis reaction.

For untreated MBW, the measured total reducing sugar content was 0.78 mg mL^{-1} (Fig. 8). In the batch bioreactor, the production of reducing sugar increased to 1.17 mg mL^{-1} for $\text{RES}_{\text{batch}}^{\text{MnP}}$ and 1.36 mg mL^{-1} for $\text{RES}_{\text{batch}}^{\text{LiP}}$ (Fig. 8). These results demonstrate that lignin depolymerization by MnP and LiP in the batch bioreactor improved the hydrolysis efficiency of carbohydrates in the residue compared to untreated MBW.

In the membrane bioreactor, the production of reducing

sugar further increased to 1.80 mg mL^{-1} for $\mathrm{RES}^{\mathrm{MnP}}_{\mathrm{membrane}}$ and 2.11 mg mL^{-1} for $\mathrm{RES}^{\mathrm{LiP}}_{\mathrm{membrane}}$ (Fig. 8).

This finding suggests that lignin depolymerization by MnP and LiP in the membrane bioreactor resulted in additional enhancements in hydrolysis efficiency for the carbohydrates in the residue, surpassing both untreated MBW and the batch bioreactor.

Discussion

For the enzymatic depolymerization of grass lignin using laccase, accumulation of water-soluble lignin upon the reaction was reported by Hilgers *et al*.[16] Similar to that report, in the present study, water-soluble lignin fragments were also detected in the aqueous phase after the MnP- and LiP-catalyzed reactions in the batch bioreactor (Figs. 2a and 2b). Therefore, both MnP and LiP used in this study successfully catalyzed the lignin depolymerization to produce water-soluble lignin fragments. However, such lignin fragments produced through enzymatic depolymerization are reportedly highly reactive and hence undergo a series of complex reactions, which leads to either further depolymerization of lignin chains, or radical recoupling resulting in lignin repolymerization.[46-48] Thereby, the yield of the lignin fragments in the batch bioreactor was supposed to be highly dependent on the balance between depolymerization and repolymerization. To overcome this problem, we used the membrane bioreactor to continuously isolate the reactive lignin fragments to enhance the lignin depolymerization efficiency. As expected, the total amounts of water-soluble lignin fragments significantly increased with the membrane bioreactor, 28-fold for MnP and 18-fold for LiP, respectively (Fig. 2g), indicating that the isolation of lignin fragments could increase the efficiency of lignin depolymerization.

The GC-MS analysis on M_19 in the filtrate fractions revealed the presence of depolymerized products produced by either MnP- or LiP-catalyzed depolymerization of MBW, which were subsequently isolated from the reaction vessel through the membrane (Table 1). Among the products, monomeric aromatic compounds such as syringol and vanillin have various industrial applications. This makes the continuous isolation of these fine chemicals from the reaction vessel through the membrane desirable especially for large-scale biocatalytic lignin depolymerization process. However, it should be noted that the use of a membrane bioreactor is associated with lower concentrations of the targeted products due to the larger reaction volumes involved. Although we successfully detected the presence of these fine chemicals using a high-sensitivity GC-MS system, it was still necessary to concentrate M_19 for accurate GC-MS analysis. Therefore, further research is necessary to develop a more cost-effective method for the efficient separation and purification of these products, ultimately enhancing their overall yield.

The quantification of lignin in RES showed a decrease in LP of MBW due to MnP- and LiP-catalyzed reactions. A higher degree of lignin removal was achieved in the membrane bioreactor relative to in the batch bioreactor for both MnP and LiP (Fig. 3 and Table 2). These results suggested that the aforementioned higher production of water-soluble lignin fragments in the membrane bioreactor led to the greater lignin removal from MBW. Additionally, the quantification of lignin in RES indicated a significant improvement in the efficiency of lignin depolymerization achieved by the membrane bioreactor.

Upon the MnP- and LiP-catalyzed reactions, a reduction in the HML proportion for RES was observed (Fig. 4 and Table 3). This finding suggests the depolymerization of HML by both MnP and LiP. The reduction was more significant for the membrane bioreactor than for the batch bioreactor. These observations further supported that the efficiency of lignin depolymerization was highly improved by the membrane bioreactor.

Compared to untreated MBW, the increase in the amounts of reducing sugar produced from MBW after treatment with MnP and LiP in both batch and membrane bioreactors indicates the positive effect of reduced lignin content in the sample on enhancing the hydrolysis efficiency of lignocellulosic biomass. Notably, the hydrolysis efficiency of sample obtained from the membrane bioreactor is higher than those from the batch bioreactor. This observation aligns with findings from a previous study, where the improved hydrolysis yield was attributed to the enhanced accessibility of carbohydrates to the hydrolytic enzymes.[49] These results underscore the possible application of RES obtained after treatment with MnP and LiP, particularly for membrane bioreactor, as a promising approach for efficient lignocellulosic biomass hydrolysis.

In this study, our primary objective was to investigate the potential advantages of continuous separation of lignin fragments from the reaction medium using a membrane bioreactor, in comparison to a conventional batch bioreactor. Thus, we employed a lower biomass loading to ensure proper biomass dispersion in the reaction vessel and faster separation of lignin fragments through the membrane. Although we did not specifically examine the standard conditions utilized in industrial batch-scale processes, we anticipate that an improvement in lignin depolymerization would likely be observed under such industrial reaction conditions as well.

Upon the MnP- and LiP-catalyzed reactions, a reduction in the M_w of HML for RES was also observed (Fig. 4 and Table 3). The reduction was more significant for the membrane bioreactor as well than for the batch bioreactor. This is another indication of the higher efficiency of lignin depolymerization by the membrane bioreactor. We did not insist that our system reduced the condensation of lignin. We did not argue whether the amount of the condensation of lignin formed through the C-C' bonds increases or not, by our system. Our intention was to propose the enhanced depolymerization of lignin and its removal by our system on the basis of the SEC profile (Fig. 4) and quantification of lignin by Klason lignin/UV-vis spectroscopy lignin (Table 2), respectively.

The NMR spectroscopic analysis of RES also demonstrated the enhanced lignin removal by the membrane bioreactor, because a more drastic reduction in the lignin signal volume was observed for the membrane bioreactor than for the batch bioreactor (Figs. 5 and 6). It is noteworthy that the solubilities of the samples in DMSO may vary due to their different

chemical compositions. Even though we used the same sample preparation method, if the residues obtained from the membrane bioreactor had lower solubility in DMSO, this could have also contributed to the lower lignin signal intensity observed in the NMR spectra. As a result, there may have been an underestimation of the relative amount of lignin substructures, which may result in an overestimation of lignin removal.

As far as the spectra observed are concerned, the extent of the reduction in signal volume does not drastically differ between the interunit linkage and aromatic regions (Fig. 7). This means aromatic rings of lignin are not cleaved by the reaction. Additionally, NMR analysis of lignin substructures suggested that no notable structural modification occurred for the lignin remaining in RES. It is deduced that most of the remaining lignin in RES still maintains its native structure.

For the membrane bioreactor, MnP- and LiP-catalyzed reactions were compared. Firstly, the lignin removal was more effective for the LiP-catalyzed reaction (Fig. 3 and Table 2). Secondly, the reduction in the HML proportion was more drastic for the LiP-catalyzed reaction (Table 3). LiP seems to be superior to MnP.

In addition to the lignin repolymerization issue, acquiring a large quantity of peroxidase for biological lignin valorization is another task to be overcome.[26] Heterologous expression using a yeast like *Pichia pastoris* is generally superior to homologous expression in terms of large-scale protein production. In this study, lignin depolymerization was successfully achieved with heterologously expressed peroxidases. Furthermore, these peroxidases had the ability to depolymerize lignin even without costly purification and at a low enzyme load relative to the reported enzymatic lignin removal.[15-17] These results imply that enzymatic depolymerization is an applicable approach for economical biomass utilization.

Conclusion

In summary, we demonstrated the advantage of the membrane bioreactor for lignin depolymerization through the peroxidase-catalyzed reaction. The isolation of lignin fragments using the membrane bioreactor can significantly enhance the depolymerization of beech wood lignin and its removal. To the best of our knowledge, this is the first report of a significant enhancement of biocatalytic lignin depolymerization of a natural lignocellulosic biomass realized with a membrane bioreactor using MnP and LiP. Furthermore, while our investigation focused on the enzymatic aspect, we firmly believe that the membrane bioreactor concept holds promise for broader applications in lignin conversion, including chemical processes.

Additionally, the enhanced lignin removal from MBW in membrane bioreactors catalyzed by either MnP or LiP must be favorable from the biorefinery perspective, where a lesser inhibitory effect of lignin on the saccharification of carbohydrates is expected, ultimately yielding a higher saccharification efficiency. Overall, the enzymatic reaction carried out with continuous isolation of reactive lignin fragments should be a huge milestone towards a sustainable yet efficient biorefinery.

Author Contributions

Kenneth Sze Kai Teo: Conceptualization, Methodology, Validation, Formal analysis, Investigation, Writing – Original Draft, Writing – Review & Editing, Visualization. **Keiko Kondo:** Conceptualization, Methodology, Validation, Formal analysis, Investigation, Writing – Review & Editing, Visualization, Funding acquisition. **Kaori Saito:** Methodology. **Yu Iseki:** Methodology. **Takashi Watanabe:** Methodology. **Takashi Nagata:** Conceptualization, Methodology, Validation, Formal analysis, Investigation, Writing – Review & Editing, Visualization, Supervision, Funding acquisition. **Masato Katahira:** Conceptualization, Methodology, Validation, Formal analysis, Investigation, Writing – Original Draft, Writing – Review & Editing, Visualization, Supervision, Funding acquisition.

Conflicts of interest

There are no conflicts of interest to declare.
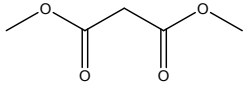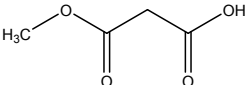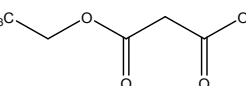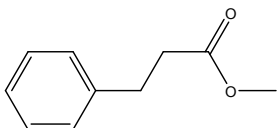
Acknowledgements
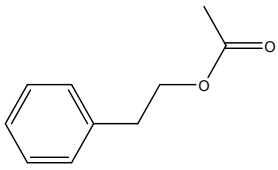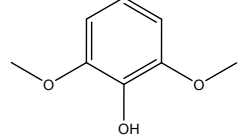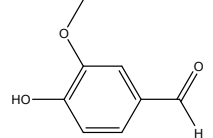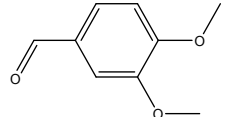
Notes and references

1   J. Cai, Y. He, X. Yu, S. W. Banks, Y. Yang, X. Zhang, Y. Yu, R. Liu and A. V. Bridgwater, *Renewable Sustainable Energy Rev.*, 2017, **76**, 309-322.
2   S. Liu, *Biotechnol. Adv.*, 2010, **28**, 563-582.
3   L. M.C. L. K. Curran, L. T. M. Pham, K. L. Sale and B. A. Simmons, *Biotechnol. Adv.*, 2022, **54**, 107809.
4   M. Xie, J. Zhang, T. J. Tschaplinski, G. A. Tuskan, J. Chen and W. Muchero, *Front. Plant Sci.*, 2018, **9**, 1427.
5   V. K. Ponnusamy, D. D. Nguyen, J. Dharmaraja, S. Shobana, J. R. Banu, R. G. Saratale, S. W. Chang and G. Kumar, *Bioresour. Technol.*, 2019, **271**, 462-472.
6   E. M. Anderson, M. L. Stone, R. Katahira, M. Reed, W. Muchero, K. J. Ramirez, G. T. Beckham and Y. Román-Leshkov, *Nat. Commun.*, 2019, **10**, 2033.
7   J. Barros, L. Escamilla-Trevino, L. Song, X. Rao, J. C. Serrani-Yarce, M. D. Palacios, N. Engle, F. K. Choudhury, T. J. Tschaplinski, B. J. Venables, R. Mittler and R. A. Dixon, *Nat. Commun.*, 2019, **10**, 1994.
8   Q. Liu, L. Luo and L. Zheng, *Int. J. Mol. Sci.*, 2018, **19**, 235.
9   S. Guadix-Montero and M. Sankar, *Top. Catal.*, 2018, **61**, 183-198.
10 Y. Jian, Y. Meng and H. Li, *Front. Energy Res.*, 2022, **9**, 827680.
11 H. B. Aditiya, T. M. I. Mahlia, W. T. Chong, H. Nur and A. H. Sebayang, *Renewable Sustainable Energy Rev.*, 2016, **66**, 631-653.

12 Y. Su, X. Yu, Y. Sun, G. Wang, H. Chen and G. Chen, *Sci. Rep.*, 2018, **8**, 5385.
13 R. C. Wilhelm, R. Singh, L. D. Eltis and W. W. Mohn, *ISME J.* 2019, **13**, 413-429.
14 T. Cui, B. Yuan, H. Guo, H. Tian, W. Wang, Y. Ma, C. Li and Q. Fei, *Biotechnol. Biofuels Bioprod.*, 2021, **14**, 162.
15 A. Rico, J. Rencoret, J. C. d. Río, A. T. Martínez and A. Gutiérrez, *Biotechnol. Biofuels Bioprod*, 2014, **7**, 6.
16 R. Hilgers, G. v. Erven, V. Boerkamp, I. Sulaeva, A. Potthast, M. A. Kabel and J. Vincken *Green Chem.*, 2020, **22**, 1735-1746.
17 J. Rencoret, A. Pereira, J. C. d. Río, A. T. Martínez and A. Gutiérrez, *BioEnergy Res.*, 2016, **9**, 917-930.
18 L. Munk, A. M. Punt, M. A. Kabel and A. S. Meyer, *RSC Adv.*, 2017, **7**, 3358-3368.
19 P. Baiocco, A. M. Barreca, M. Fabbrini, C. Galli and P. Gentili, *Org. Biomol. Chem.*, 2003, **1**, 191-197.
20 L. Munk, A. K. Sitarz, D. C. Kalyani, J. D. Mikkelsen and A. S. Meyer, *Biotechnol. Adv.*, 2015, **33**, 13-24.
21 P. Nousiainen, J. Kontro, H. Manner, A. Hatakka and J. Sipilä, *Fungal Genet. Biol.*, 2014, **72**, 137-149.
22 E. Fernández-Fueyo, F. J. Ruiz-Dueñas and A. T. Martínez, *Biotechnol. Biofuels Bioprod.*, 2017, **7**, 114.
23 T. Jian, Y. Zhou, P. Wang, W. Yang, P. Mu, X. Zhang, X. Zhang and C. Chen *Nat. Commun.*, 2022, **13**, 3025.
24 B. M. Majeke, F. Collard, L. Tyhoda and J. F. Görgens, *Bioresour. Technol.*, 2021, **319**, 124152.
25 E. Liu, F. Segato, R. A. Prade and M. R. Wilkins, *Bioresour. Technol.*, 2021, **338**, 125564.
26 H. Xu, G. M. Scott, F. Jiang and C. Kelly, *Holzforschung*, 2010, **64**, 017.
27 C. Cagide and S. Castro-Sowinski, *Environ. Sustainability*, 2020, **3**, 371-389.
28 T. Warinowski, S. Koutaniemi, A. Kärkönen, I. Sundberg, M. Toikka, L. K. Simola, I. Kilpeläinen and T. H. Teeri, *Front. Plant Sci.*, 2016, **7**, 01523
29 X. Mu, Z. Han, C. Liu and D. Zhang, *J. Phys. Chem. C*, 2019, **123**, 8640-8648.
30 S. Dabral, J. Engel, J. Mottweiler, S. S. M. Spoehrle, C. W. Lahive and C. Bolm, *Green Chem.*, 2018, **20**, 170-182.
31 P. J. Deuss, C. S. Lancefield, A. Narani, J. G. de Vries, N. J. Westwood and K. Barta, *Green Chem.*, 2017, **19**, 2774-2782.
32 O. Yu, C. G. Yoo, C. S. Kim and K. H. Kim, *ACS Omega*, 2019, **4**, 16103-16110.
33 N. Li, Y. Li, C. G. Yoo, X. Yang, X. Lin, J. Ralph and X. Pan, *Green Chem.*, 2018, **20**, 4224-4235.
34 V. Steinmertz, M. Villain-gambier, A. Klem, I. Ziegler, S. Dumarcay and D. Trebouet, *Bioresour. Technol.*, 2020, **311**, 123530.
35 M. Lin, T. Nagata and M. Katahira, *Protein Expression Purif.*, 2018, **145**, 45-52.
36 M. M. Abu-Omar, K. Barta, G. T. Beckham, J. S. Luterbacher, J. Ralph, R. Rinaldi, Y. Román-Leshkov, J. S. M. Samec, B. F. Sels and F. Wang, *Energy Environ. Sci.*, 2021, **14**, 262-292.
37 A. Sluiter, B. Hames, R. Ruiz, C. Scarlata, J. Sluiter, D. Templeton, and D. Crocker, Determination of structural carbohydrates and lignin in biomass, Report NREL/TP-510-42618, National Renewable Energy Laboratory, Golden, CO, USA, 2012.
38 H. Zhang, H. Zhao, Y. Yang, H. Ren and H. Zhai, *Green Chem.*, 2022, **24**, 2212-2221.
39 D. Mikulski and G. Kłosowski, *Sci. Rep.*, 2022, **12**, 4561.
40 S. D. Mansfield, H. Kim, F. Lu and J. Ralph, *Nat. Protoc.*, 2012, **7**, 1579-1589.
41 J. del Río, J. Rencoret, P. Prinsen, A. T. Martínez, J. Ralph and A. Gutiérrez, *J. Agric. Food Chem.*, 2012, **60**, 5922-5935.
42 J. Rencoret, P. Prinsen, A. Gutiérrez, A. T. Martínez and J. del Río, *J. Agric. Food Chem.*, 2015, **63**, 603-613.
43 T. Yuan, S. Sun, F. Xu and R. Sun, *J. Agric. Food Chem.*, 2011, **59**, 10604-10614.
44 G. L. Miller, *Anal. Chem.*, 1959, **31**, 3, 426-428.
45 S. Zhang, Z. Dong, J. Shi, C. Yang, Y. Fang, G. Chen and C. Tian, *Bioresour. Technol.*, 2022, **361**, 127699.
46 D. Salvachúa, R. Katahira, N. S. Cleveland, P. Khanna, M. G. Resch, B. A. Black, S. O. Purvine, E. M. Zink, A. Prieto, M. J. Martínez, A. T. Martínez, B. A. Simmons, J. M. Gladden and G. T. Beckham, *Green Chem.*, 2016, **18**, 6046-6062.
47 T. D. H. Bugg and R. Rahmanpour, *Curr. Opin. Chem. Biol.*, 2015, **29**, 10-17.
48 H. Son, H. Seo, S. Han, S. M. Kim, L. T. M. Pham, M. F. Khan, H. J. Sung, S. Kang, K. Kim and Y. H. Kim, *Enzyme Microb. Technol.*, 2021, **148**, 109803.
49 M. Nazar, L. Xu, M. W. Ullah, J. M. Moradian, Y. Wang, S. Sethupathy, B. Iqbal, M. Z. Nawaz and D. Zhu, *J. Clean. Prod.*, 2022, **360**, 132171.

Table 1 The main depolymerized products of beech wood lignin obtained in the filtrate fraction

| No.	Structural formula	Name	Molecular formula	Involved enzyme
1		Propanedioic acid, dimethyl ester	$C_5H_8O_4$	LiP
2		Monomethyl malonate	$C_4H_6O_4$	LiP
3		Ethyl hydrogen malonate	$C_5H_8O_4$	MnP LiP
4		Benzenepropanoic acid, methyl ester	$C_{10}H_{12}O_2$	MnP LiP
5		Acetic acid, 2-phenylethyl ester	$C_{10}H_{12}O_2$	MnP LiP
6		Syringol	$C_8H_{10}O_3$	MnP
7		Vanillin	$C_8H_8O_3$	MnP LiP
8		Veratryl aldehyde	$C_9H_{10}O_3$	LiP

Table 2 Quantification of lignin in solid residues (RES)[a]

| Sample	Klason lignin (%)	UV-vis spectroscopy lignin (%)	Change in LP (%)[b]	
			Klason lignin	UV-vis lignin
MBW	24.5 ± 0.4	26.9 ± 0.3	-	-
Batch bioreactor				
No enzyme	22.8 ± 0.4	26.8 ± 0.3	−6.9 ± 0.8	−0.4 ± 1.0
MnP	21.4 ± 0.6	22.3 ± 0.7	−12.6 ± 0.9	−17.3 ± 1.7
LiP	19.8 ± 0.3	19.4 ± 0.9	−19.2 ± 0.8	−27.7 ± 2.5
Membrane bioreactor				
No enzyme	22.9 ± 0.2	26.8 ± 0.3	−6.6 ± 0.8	−0.1 ± 2.1
MnP	16.9 ± 0.6	16.2 ± 0.5	−31.1 ± 2.4	−39.7 ± 1.7
LiP	14.3 ± 0.5	14.2 ± 1.0	−41.5 ± 1.9	−46.7 ± 3.4

[a]Means ± SD (standard deviation) were obtained from technical duplicates. [b]Change in percentage of lignin (LP) was calculated according to Eq. (3).

Table 3 Molecular weight analysis of HML and LML fractions based on SEC of acetylated CEL obtained from solid residues (RES) of MBW

| Sample	Fraction	%	M_w (g mol^{-1})	M_n (g mol^{-1})	PDI (M_w/M_n)
MBW	HML	88.2	11336	5497	2.1
	LML	11.8	224	151	1.5
Batch bioreactor					
No enzyme	HML	90.7	11090	5466	2.0
	LML	9.3	213	153	1.4
MnP	HML	68.0	7968	5059	1.6
	LML	32.0	243	172	1.4
LiP	HML	74.3	8501	5102	1.7
	LML	25.7	232	174	1.3
Membrane bioreactor					
No enzyme	HML	89.8	11890	5922	2.0
	LML	10.2	218	153	1.4
MnP	HML	62.6	6155	4416	1.4
	LML	37.4	255	182	1.4
LiP	HML	49.0	6313	4518	1.4
	LML	51.0	235	169	1.4
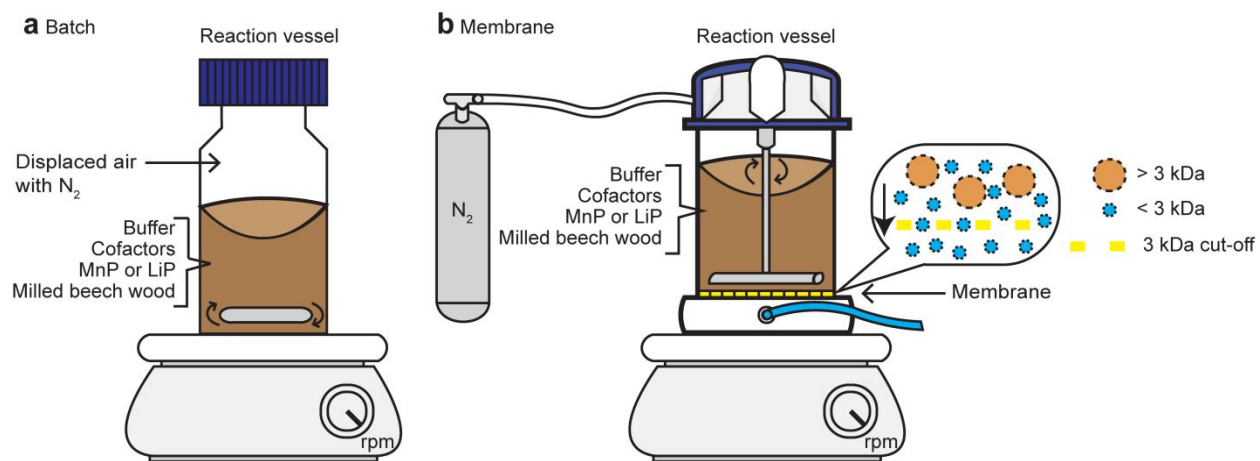
Fig. 1 Schematic drawing of bioreactors used for the enzymatic reaction. (a) Batch bioreactor. (b) Membrane bioreactor.
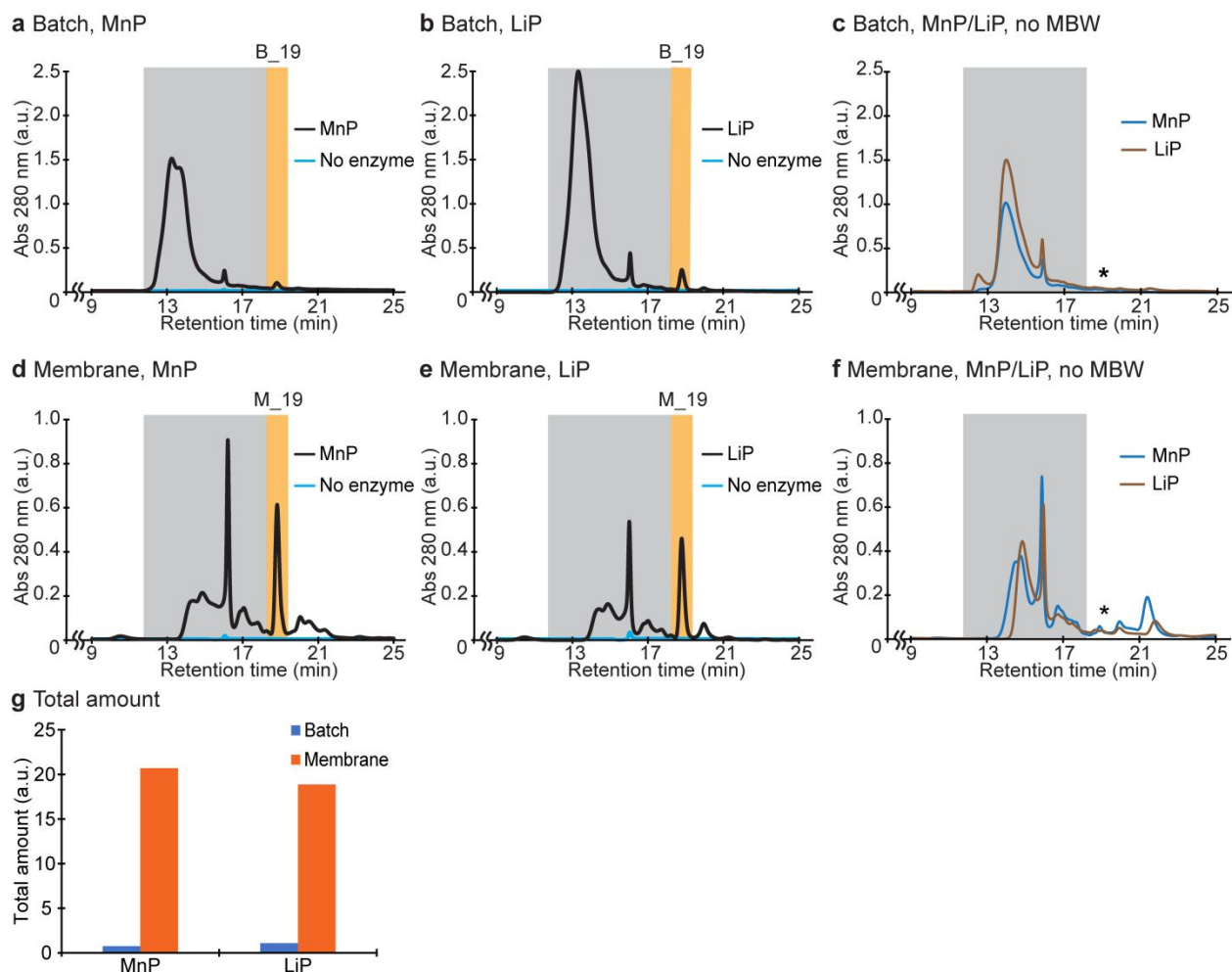
Fig. 2 SEC analyses of the reaction products released into the aqueous phase of milled beech wood (MBW) treated with peroxidases in batch and membrane bioreactors. (a-c) The SEC profiles for the reaction products released into the aqueous phase for the batch bioreactor. MBW was reacted with either MnP (a) or LiP (b) for 8 h. The cyan lines in (a) and (b) are controls; MBW was incubated without an enzyme for 8 h. Either MnP or LiP was also incubated without MBW for 8 h (c), which is also a control. (d-f) The SEC profiles for the reaction products released into the aqueous phase for the membrane bioreactor. MBW was reacted with either MnP (d) or LiP (e), and for each of them, the SEC profile of the filtrate collected after 1 hour is shown. The cyan lines in (d) and (e) are controls; MBW incubated without an enzyme and filtrate was collected after 1 h. Either MnP or LiP was incubated without MBW and the filtrates were collected after 1 h (f), which were also controls. The major peak at 18.8 min is highlighted in orange. The asterisks in (c) and (f) denote the position of B_19 and M_19, respectively. Peaks highlighted in gray are not of interest

as they were also detected for the control sample without MBW. (g) The total amounts for B_19 and M_19 estimated according to Eqs. (1) and (2).
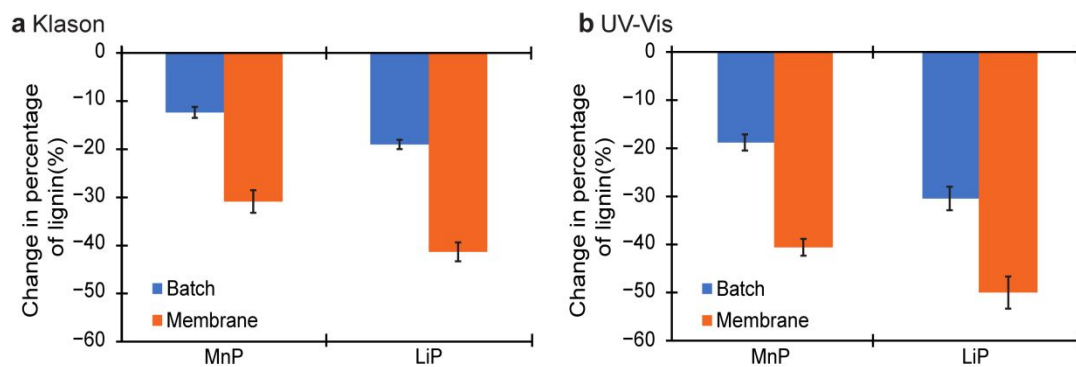
Fig. 3 The change in percentage of lignin (LP) of MBW achieved through peroxidase treatment in the batch and membrane bioreactors. (a and b) The change in LP achieved through the MnP and LiP treatments, which was calculated using Eq. (3), based on the LP of the initial MBW and the LP after the treatment with a peroxidase. The LP was determined by the Klason lignin (a) and UV-Vis spectroscopy (b) methods.
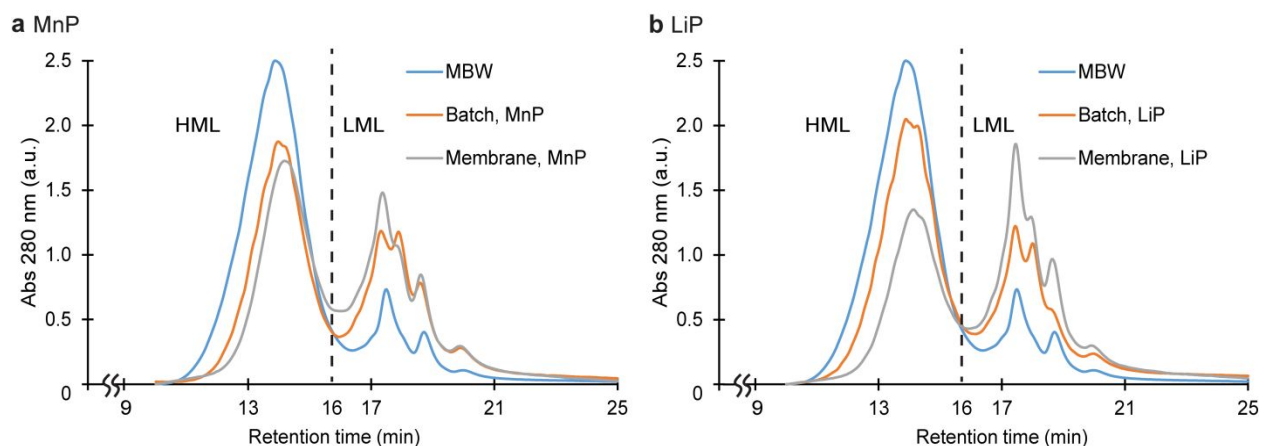
Fig. 4 Molecular weight distributions of lignin in the solid residue (RES) after peroxidase treatment of MBW. (a) SEC profiles of the acetylated cellulolytic enzyme lignin (CEL) extracted from the RES after treatment with MnP in batch (RES$_{batch}^{MnP}$, orange line) and membrane (RES$_{membrane}^{MnP}$, gray line) bioreactors. (b) SEC profiles of the acetylated CEL extracted from the RES after treatment with LiP in the batch (RES$_{batch}^{LiP}$, orange line) and membrane (RES$_{membrane}^{LiP}$, gray line) bioreactors. SEC profiles of the acetylated CEL extracted from the initial MBW supplied to the bioreactors are presented in (a) and (b) (blue line). The high molecular weight lignin (HML) and low molecular weight lignin (LML) fractions are defined as lignin with molecular weights greater and lower than 1000 (elution time at 16 min, dotted line), respectively.
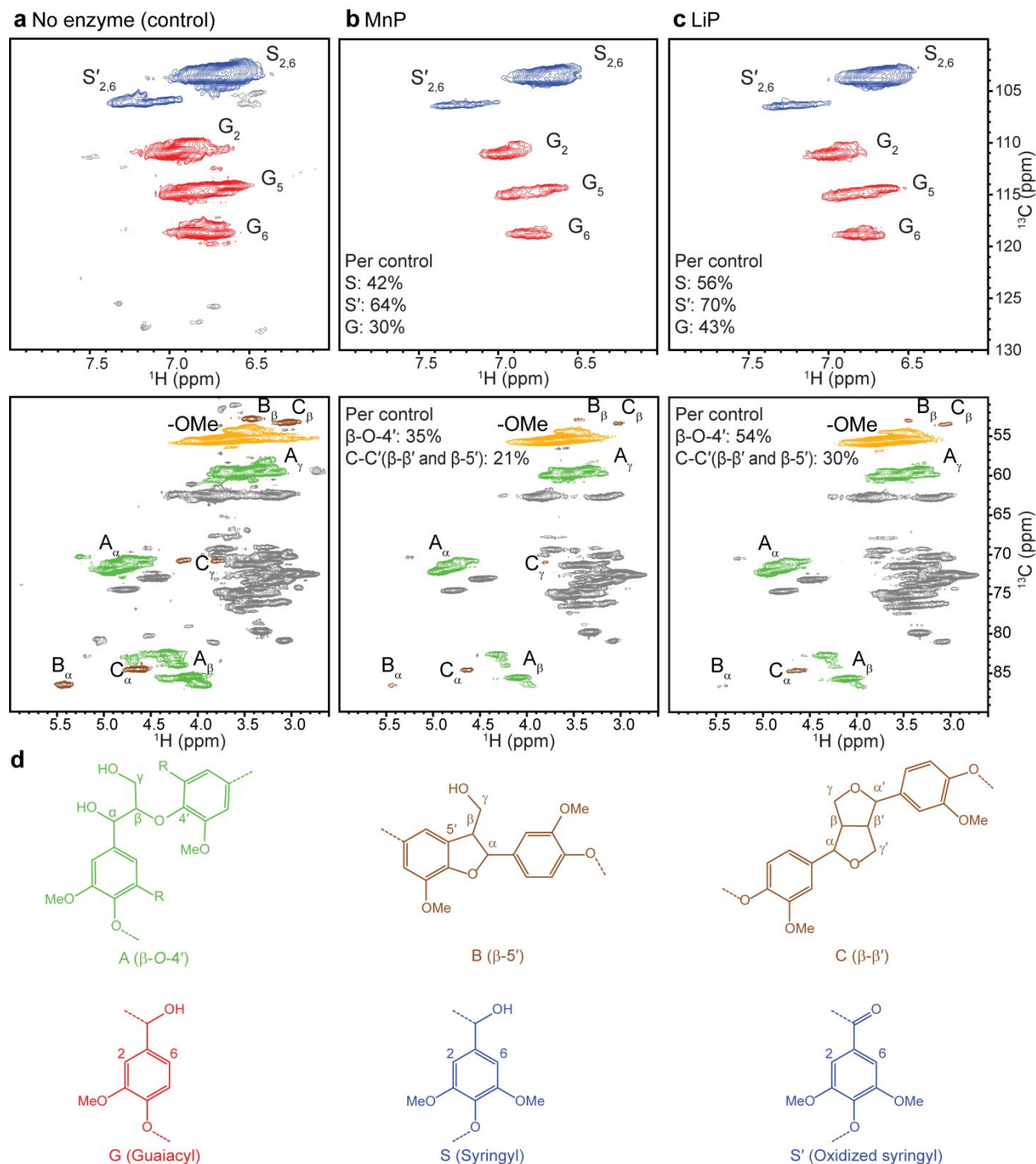
Fig. 5 NMR analysis of RES after the peroxidase treatment in the batch bioreactor. (a-c) 2D ^{1}H-^{13}C HSQC spectra of the RES obtained after the treatment of MBW with the batch bioreactor in three different solution conditions; no enzyme (a), and with either MnP (b) or LiP (c). The upper and lower panels in (a-c) are the aliphatic and aromatic regions of each HSQC spectrum, respectively. (d) The main lignin substructures identified in HSQC spectra, which are color-coded

as for the spectra. Gray signals represent unassigned signals, which mainly originated from polysaccharides. A complete list of the identified substructures can be found in Supplementary Table S2. Relative amounts of lignin substructures (S, G, S′, β-O-4′ and C-C′) in RES obtained after treatment with MnP (a) and LiP (b) relative to RES treated without an enzyme determined by Eq. (4).
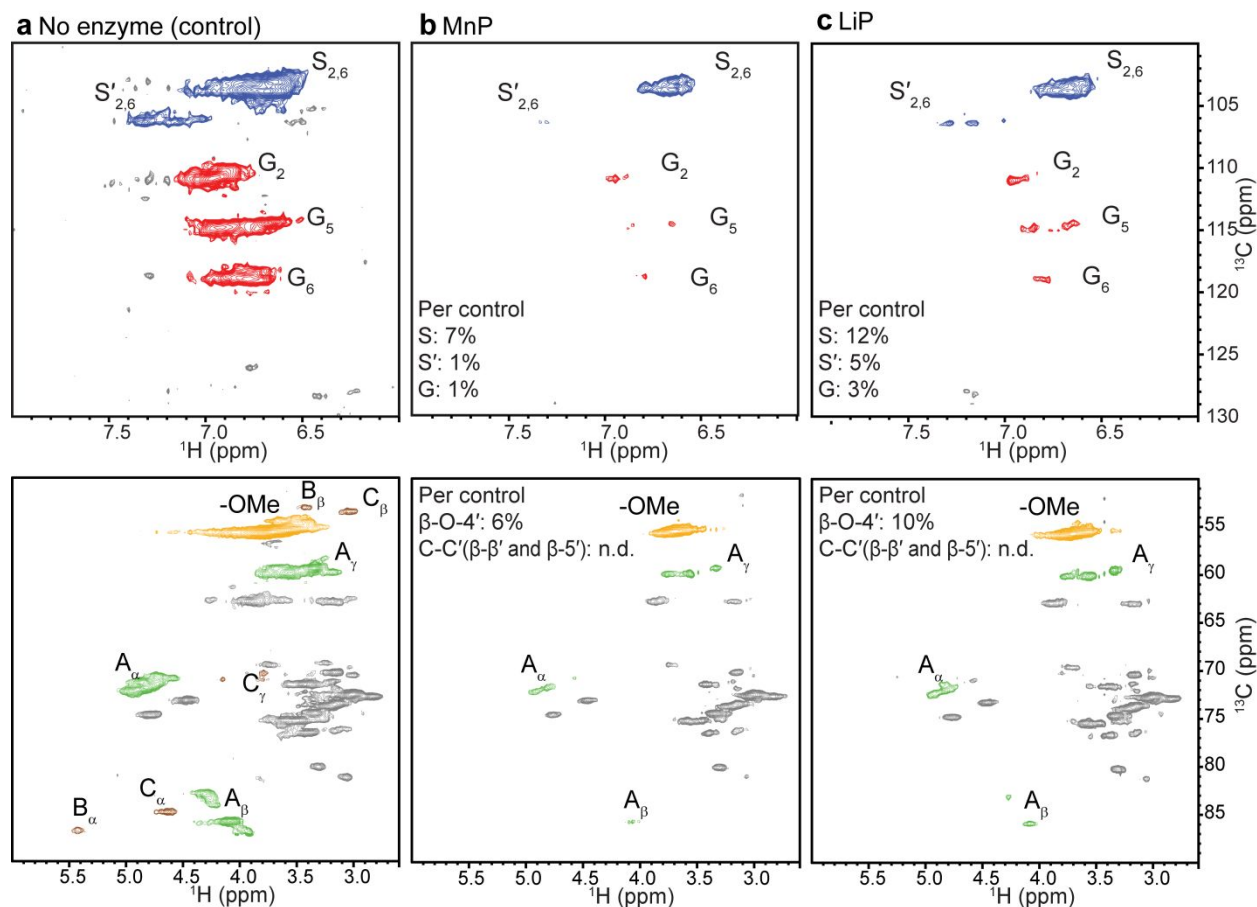
Fig. 6 NMR analysis of RES after the peroxidase treatment in the membrane bioreactor. 2D ^{1}H-^{13}C HSQC spectra of the RES obtained after the treatment of MBW with the membrane bioreactor in three different solution conditions; no enzyme (a), and with either MnP (b) or LiP (c). The upper and lower panels in (a-c) are the aliphatic and aromatic regions of each HSQC spectrum, respectively. Gray signals represent unassigned signals, which mainly originated from polysaccharides. Relative amounts of lignin substructures (S, G, S′, β-O-4′ and C-C′) in RES obtained after treatment with MnP (a) and LiP (b) relative to RES treated without an enzyme determined by Eq. (4).
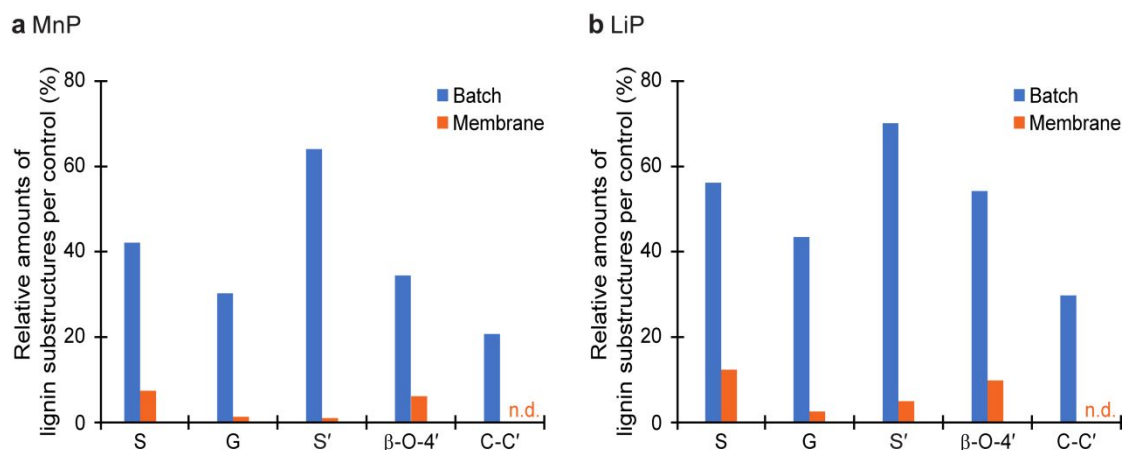
Fig. 7 Semi-quantitative analysis of the lignin substructures on the basis of 2D ^{1}H-^{13}C HSQC experiments. (a and b) Relative amounts of lignin substructures (S, G, S′, β-O-4′ and C-C′) in RES obtained after treatment with MnP (a) and LiP (b) relative to RES treated without an enzyme determined by Eq. (4). The relative amount was determined based on the volume integrals of the HSQC correlation peaks. The amounts of β-O-4′ and C-C′ (β-β′ and β-5′) interunit linkages were estimated on the basis of the volume of the C_α-H_α correlation. The amounts of S- and S′-units were estimated from the half values of the volumes of the $C_{2,6}$-$H_{2,6}$ correlation, whereas that of the G-unit was estimated from the volume of the C_2-H_2 correlation. n.d.; not detected.
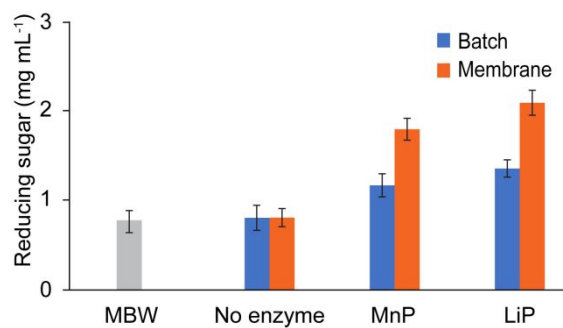
Fig. 8 The reducing sugar released from the hydrolysis of MBW and RES obtained from batch and membrane bioreactors. Error bars show the standard deviation of three replicates.